

# Reference electrode-induced surface poisoning of thin-film electrodes

***Citation for published version (APA):***

Niessen, R. A. H., & Notten, P. H. L. (2005). Reference electrode-induced surface poisoning of thin-film electrodes. *Journal of the Electrochemical Society*, 152(10), A2051-A2057. <https://doi.org/10.1149/1.2034521>

***DOI:***

[10.1149/1.2034521](https://doi.org/10.1149/1.2034521)

***Document status and date:***

Published: 01/01/2005

***Document Version:***

Publisher's PDF, also known as Version of Record (includes final page, issue and volume numbers)

***Please check the document version of this publication:***

- A submitted manuscript is the version of the article upon submission and before peer-review. There can be important differences between the submitted version and the official published version of record. People interested in the research are advised to contact the author for the final version of the publication, or visit the DOI to the publisher's website.
- The final author version and the galley proof are versions of the publication after peer review.
- The final published version features the final layout of the paper including the volume, issue and page numbers.

[Link to publication](#)

***General rights***

Copyright and moral rights for the publications made accessible in the public portal are retained by the authors and/or other copyright owners and it is a condition of accessing publications that users recognise and abide by the legal requirements associated with these rights.

- Users may download and print one copy of any publication from the public portal for the purpose of private study or research.
- You may not further distribute the material or use it for any profit-making activity or commercial gain
- You may freely distribute the URL identifying the publication in the public portal.

If the publication is distributed under the terms of Article 25fa of the Dutch Copyright Act, indicated by the "Taverne" license above, please follow below link for the End User Agreement:

[www.tue.nl/taverne](http://www.tue.nl/taverne)

***Take down policy***

If you believe that this document breaches copyright please contact us at:

[openaccess@tue.nl](mailto:openaccess@tue.nl)

providing details and we will investigate your claim.



## Reference Electrode-Induced Surface Poisoning of Thin-Film Electrodes

R. A. H. Niessen<sup>a,z</sup> and P. H. L. Notten<sup>a,b,\*</sup>

<sup>a</sup>Eindhoven University of Technology, 5600 MB Eindhoven, The Netherlands

<sup>b</sup>Philips Research Laboratories, 5656 AA Eindhoven, The Netherlands

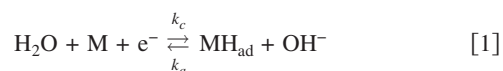
The effect of reference electrode (RE)-induced surface poisoning of magnesium–scandium (MgSc) thin-film electrodes has been investigated. A comparison is made between various electrochemical responses of identical MgSc thin-film electrodes. The measurements were performed in two separate three-electrode setups containing REs from different manufacturers, the first of which contained a radiometer Hg/HgO RE that consists of a glass construction. The second setup contained a Hg/HgO RE from Koslow Scientific Company, which has a polyethylene housing. It was found that lead (Pb) species originating from the radiometer RE readily dissolves into the alkaline electrolyte. These dissolved species could be deposited on the surface of thin film electrodes, both as metallic Pb and Pb oxides, during electrochemical hydrogen loading/unloading of the MgSc alloys. This surface poisoning prohibits accurate determination of kinetic parameters related to the hydrogen adsorption reaction. The electrochemical measurements showed inferior electrode kinetics when using a radiometer RE as compared to a Koslow RE. The electrode kinetics could be linked directly to the amount of Pb deposited on the metal hydride thin film by means of electrochemical impedance spectroscopy and analytical techniques.

© 2005 The Electrochemical Society. [DOI: 10.1149/1.2034521] All rights reserved.

Manuscript submitted February 7, 2005; revised manuscript received June 6, 2005. Available electronically August 25, 2005.

After the discovery in 1996 that hydrogenation of thin films comprised of rare earth metals resulted in striking optical transitions, intensive research was initiated in this field.<sup>1–5</sup> These rare earth thin films can be switched from transparent in the fully hydrogen loaded state (where it is a semiconductor) to nontransparent in the hydrogen-depleted (metallic) state, just by changing the hydrogen concentration. Second-generation switchable mirror materials, consisting of rare earth materials alloyed with Mg, are even able to reach a reflecting state in their low-hydrogen state.<sup>6</sup> This means that electrochromic devices based on these alloys also have the ability to serve as a shutter, aside from the variable transmission window.

Hydrogenation of metal hydride (MH) thin films can be achieved by means of gas-phase or electrochemical loading. In order to catalyze the hydrogen sorption often a palladium (Pd) topcoat is used. This Pd not only acts as a catalyst, but also slows down corrosion of the underlying MH film. However, gas-phase switching seems not to be the most logical solution in many cases, as the precise hydrogen content in the films is difficult to control and highly reactive hydrogen gas is involved. For research purposes this method is actually preferred due to its ease of use. Electrochemically induced optical switching would be ideal for both research and application purposes, as it is possible to accurately control the hydrogen content. Simplified, electrochemical hydrogen loading of a MH thin film can be described by a two-step mechanism.<sup>7</sup> The first step is the charge-transfer reaction at the solid/electrolyte interface, which can be represented by



The kinetics of this reaction is strongly dependent on the nature of the electrode surface. Once adsorbed hydrogen atoms ( $\text{H}_{\text{ad}}$ ) are formed at the electrode surface, they are absorbed ( $\text{H}_{\text{abs}}$ ) by the Pd topcoat and subsequently by the underlying MH according to



The switchable mirror materials used in optical research also exhibit high hydrogen storage capacities and are therefore excellent candidates in a wide range of applications, such as battery electrode materials<sup>8</sup> or as hydrogen storage materials for fuel cells. Thin films comprised of these materials can be advantageously used as 2D

model systems when characterizing specific material properties. The geometry of the thin-film system is especially suited for electrochemical material characterization as, for example, the interfacial area between electrolyte and solid is well defined. This subsequently enables accurate evaluation of the kinetics of the hydrogen adsorption reaction of the MH electrode under investigation. Although the geometric surface area of a thin film has a well-defined size, it is usually rather small, i.e., of the order of several square centimeters. This means that surface contamination can manifest itself rather quickly under certain circumstances, thereby severely influencing the electrochemical response of the thin-film electrode. Although in the above-mentioned thin-film research quite some effort is put into the removal of oxygen from the electrolyte,<sup>9</sup> which also has an impact on the response of a thin-film electrode, the existence of surface poisoning is generally not addressed.

Unexpectedly, electrochemical measurements using thin-film electrodes showed very different results when using identical measurement setups in which reference electrodes (REs) from different manufacturers were used. To examine this RE-induced influence, two cases are compared in this study in which similar electrochemical investigations are conducted on identical thin-film hydrogen storage electrodes. Measurements are performed using two separate three-electrode setups containing REs from different manufacturers. The first setup contains an RE constructed with a glass housing and the second an RE with a polyethylene housing. Because alkaline solutions are able to leach out contaminants embedded in glass, it is therefore expected that the first setup could be contaminated whereas the second essentially remains free of contaminants.

### Experimental

The  $\text{Mg}_{70.5}\text{Sc}_{29.5}$  thin films used in this contribution were manufactured, under high-vacuum conditions, by means of e-gun co-deposition (base pressure between  $8 \times 10^{-8}$  and  $4 \times 10^{-7}$  mbar). The 198-nm-thick films were deposited on quartz substrates ( $\varnothing$  20 mm), which were treated prior to the deposition. This treatment consisted of three steps. First, the substrates were cleaned using iso-propyl-alcohol (IPA). Hereafter an etching step followed in which the substrates were dipped in a stirred 6 M KOH solution for 5 min. Finally, after rinsing with demineralized water, the substrates were dried by placing them in an IPA vapor for 10 min. A 10-nm-thick Pd cap layer was deposited on top of the MgSc thin films also using e-gun deposition. During deposition of the alloy, the deposition rates of Mg and Sc were maintained between 0.19 and 0.52 nm s<sup>-1</sup>. Uniformity of the composition throughout the entire film was checked by means of Rutherford backscattering spectroscopy (RBS), which showed that the deposition rates were controlled

\* Electrochemical Society Active Member.

<sup>z</sup> E-mail: niessenr@natlab.research.philips.com

well. Calculations regarding the hydrogen storage capacity are solely based on the RBS measurements, of which the accuracy is around 1%. As a maximum deviation in the hydrogen storage capacity of the MgSc alloy can occur of no more than 3%, no correction is made for the Pd cap layer.

A three-electrode setup, thermostatted at 298 K by means of a water jacket, was used to electrochemically characterize the thin films. In this setup the MH thin film acted as working electrode. This electrode was contacted with a wire, which was attached to the thin film using a conductive adhesive (E-solder no. 3021 from IMI). The edges of the substrate and the contacts were coated with a chemically inert isolating lacquer (W40, Apiezon). The potential of the working electrode was measured with respect to a Hg/HgO RE filled with 6 M KOH solution. In order to minimize the ohmic drop, the tip of the RE was placed in close proximity to the working electrode. The counter electrode, a high-purity Pd rod (99.999%, Ø 5 mm, Drijfhout), was placed in a separate compartment in the cell and care was taken that the total area in contact with the electrolyte was sufficiently large. In a separate setup this counter electrode was precharged with hydrogen ( $\text{PdH}_x$ ). This was done to avoid oxygen evolution at this electrode during the measurements, which was also found to have a profound influence on the electrochemical response of the working electrode.<sup>9</sup>

Before each measurement, the entire setup was purged by vigorously bubbling oxygen-purified argon through the electrolyte in both the working and counter electrode compartments for several hours. During the electrochemical measurement the purging gas was led over instead of through the electrolyte in the working electrode compartment. This was done in order to ensure stable voltage readings of the working electrode as purging gas bubbles in the electrolyte prevent this. Oxygen-purified argon was obtained by feeding standard-grade argon through an oxygen scrubber before it was led through the electrochemical setup.<sup>9</sup>

The electrochemical measurements were conducted using two separate three-electrode setups containing REs from different manufacturers. One setup contained a radiometer XR430 Hg/HgO RE and the other a Hg/HgO RE from Koslow Scientific Company (further denoted as RE1 and RE2, respectively). The difference between both lies in the fact that RE1 consists of a glass construction, while RE2 employs a polyethylene housing. As it is known that in strong alkaline solutions contaminations embedded in glass can leach out, it is therefore expected that the first setup could be contaminated whereas the second essentially stays free of contaminants. It should be noted that the Hg, HgO, and the filling solution of both REs were analyzed to be of sufficiently high purity. Furthermore, care was taken that all other components of the setup, as well as the electrolyte, did not contain more than mere trace amounts of contaminants (not shown here).

Electrochemical experiments, such as galvanostatic measurements, galvanostatic intermittent titration technique (GITT), and electrochemical impedance spectroscopy (EIS), were all performed using an Autolab PGSTAT30 (Ecochemie B.V., Utrecht, the Netherlands). The EIS measurements were conducted at equilibrium voltage conditions using an ac amplitude of 5 mV root-mean-square (rms) and scanning the frequency from 50 kHz to 1 mHz. The EIS data were analyzed using a nonlinear least-squares fitting program (EQUIVCRT). Unless stated otherwise, the cutoff voltage applied during all galvanostatic experiments was set to 0 V vs Hg/HgO, and all potential values are given vs Hg/HgO (6 M KOH). The composition of glass components was determined by means of X-ray fluorescence (XRF), and inductively coupled plasma mass spectroscopy (ICP-MS) was used to measure the concentration of specific elements in the RE filling solutions.

## Results

Figure 1 shows the RBS spectrum of a freshly prepared sample that has not yet been electrochemically hydrided/dehydrided. It is clear that besides the response of the quartz substrate (A), only the elements are visible that were deposited by means of electron-beam

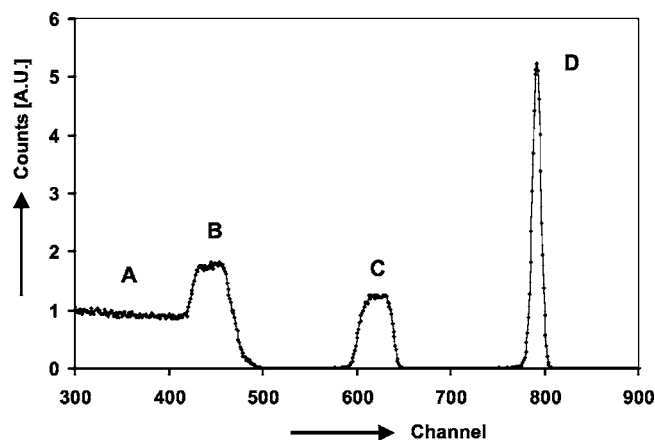


**Figure 1.** RBS spectrum of a freshly prepared MgSc thin film. The responses of interest are indicated with capitals letters: (A) quartz substrate, (B) Mg, (C) Sc, and (D) Pd.

deposition. Peaks B and C can be correlated to Mg and Sc, respectively, while peak D corresponds to Pd of the top layer. Evidently, the Pd top layer successfully protects the MgSc thin film from corrosion, as no oxygen response can be observed. Additionally, no other responses are present that point to contamination with other elements at this stage.

**Contaminated case (setup with RE1).**—The first set of electrochemical experiments was performed using the setup containing RE1. First the thin film was galvanostatically fully loaded with hydrogen using a current of  $-0.6$  mA. Subsequently, it was discharged (extraction of hydrogen) by means of GITT using a current of  $+0.12$  mA initially and  $+0.012$  mA during the last five pulses (corresponding to 938 and 93.8 mA/g, respectively). After each pulse the electrode was allowed to equilibrate for 1 h. Figure 2 shows both the obtained equilibrium curve as well as the potential response of the thin film during each current pulse. It is clear that the overpotential is increasing steadily during the GITT measurement. As demonstrated later on, this increase is not related to the concentration of hydrogen in the thin film, but to contaminants deposited onto the Pd top layer that influence the electrode kinetics.

To investigate the influence of surface poisoning on the electrode kinetics with time, the same thin-film electrode was subsequently kept at a constant potential of  $-0.925$  V for 7 days. At this potential

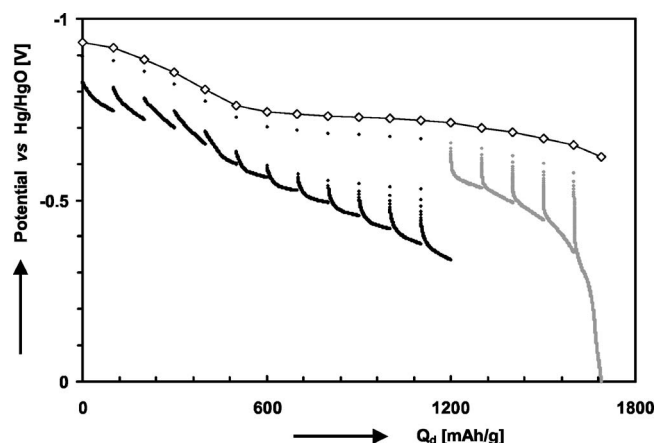


**Figure 2.** Electrochemical response of a thin-film electrode measured in a Pb-contaminated setup. Besides the equilibrium curve ( $\diamond$ ), the potential responses during every GITT pulse are shown. Current used during the GITT pulses:  $+0.12$  mA (bold line),  $+0.012$  mA (gray line).

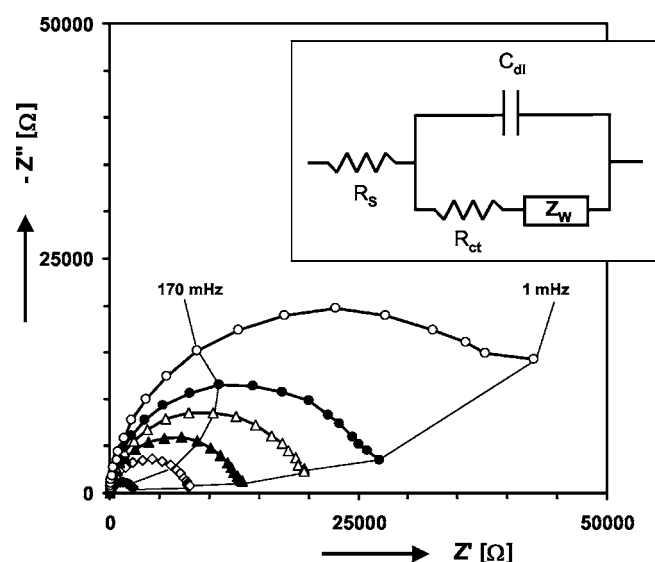


**Figure 3.** Nyquist representations of a thin film, measured in a Pb-contaminated setup, for different periods of continuous polarization at  $-0.925$  V. Polarization time: (◆) 0 days, (◇) 1 day, (▲) 2 days, (△) 3 days, (●) 4 days, and (○) 7 days. (Inset) The equivalent circuit used to model the impedance data.

the electrode remained in its fully hydrogenated state while hydrogen gas formation was kept to a minimum, as in the electrolyte used this process mainly occurs at potentials more negative than  $-0.931$  V.<sup>10</sup> At regular intervals EIS measurements were performed of which the Nyquist representations are shown in Fig. 3. Distinct semicircular impedance responses can be seen which represent the charge-transfer kinetics of the thin-film system (Reaction 1). It is evident that keeping the thin-film electrode at this negative potential ( $-0.925$  V) for a prolonged period of time causes the diameter of the semicircle to increase tremendously.

The impedance data was fitted using the electronic circuit shown in the inset of Fig. 3. This circuit is generally used to model the impedance response of a charge-transfer reaction coupled with semi-infinite diffusion of the hydrogen in the solid.<sup>11</sup> In this model the adsorption step (Reaction 2) is omitted as no apparent impedance

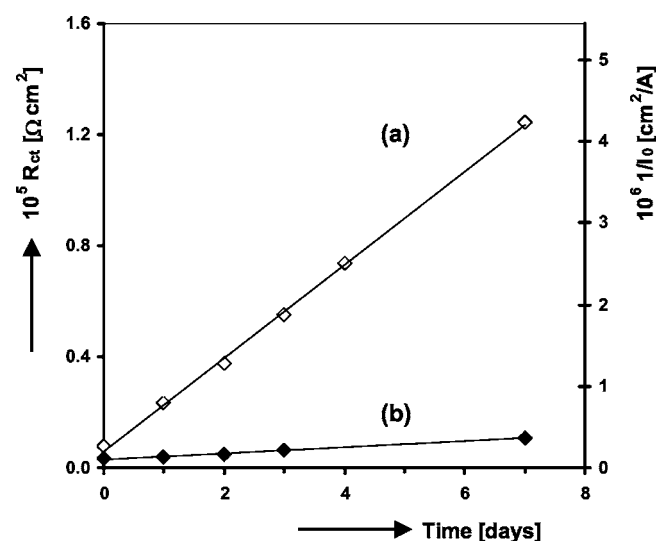


**Figure 4.** Dependency of  $R_{ct}$  and  $I_0$  vs time for identical thin-film electrodes at a constant potential of  $-0.925$  V for (a) the contaminated case and (b) contamination-free case.

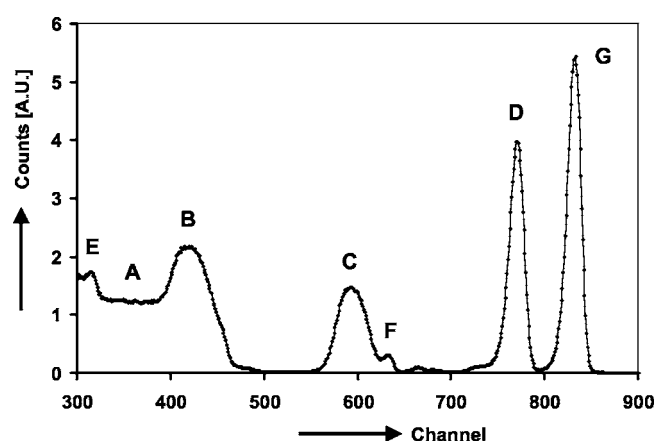


**Figure 5.** RBS spectrum of a thin-film electrode, measured in a Pb-contaminated setup, after electrochemical characterization and polarization for 7 days at  $-0.925$  V. The responses can be attributed to: (A) quartz substrate, (B) Mg, (C) Sc, (D) Pd, (E) oxygen, (F) Sc at the surface, and (G) Pb.

response could be linked to this phenomenon.<sup>12</sup> As this paper focuses on the kinetic response and not the diffusion behavior of hydrogen, the diffusion response in the EIS data is not treated. Figure 4 clearly indicates that the fitted values for the charge-transfer resistance ( $R_{ct}$ ) increase linearly with time (curve a). This shows that the charge-transfer kinetics of the thin-film electrode deteriorate severely during this potentiostatic treatment. These resistance values are also directly linked to exchange current ( $I_0$ ) via

$$R_{ct} = \frac{\eta}{i} = \frac{RT}{FI_0} \quad [3]$$

which is the low-overpotential limit of the well-known Butler-Volmer equation (see right axis of Fig. 4).<sup>13</sup>

To check the total amount of Pb deposited on the Pd topcoat of the thin film, RBS was used (see Fig. 5). The spectrum is very similar to the one shown in Fig. 1, except for the responses designated E through G. Electrochemically measuring the thin film for an extended period of time (at this stage 2 weeks in total) has led to partial oxidation of the thin-film electrode, giving a clear oxygen response (E). Judging from the position of peak F it appears that the topside of the electrode has become extremely rich in Sc. This inevitably means that the composition of the Mg and Sc in the alloy is no longer constant throughout the entire film. The most remarkable change, though, is the existence of a strong response related to deposited Pb (G). Integration of this peak shows that in total  $25 \times 10^{15}$  atoms Pb/cm<sup>2</sup> were deposited, which corresponds to about 30 monolayers of metallic Pb if complete coverage of the Pd topcoat is assumed.

**Table I.** XRF analysis of the glass housing of a radiometer XR430 Hg/HgO reference electrode.

| Main                           | Material                       | Trace | Amount (wt %) |
|--------------------------------|--------------------------------|-------|---------------|
| SiO <sub>2</sub>               |                                |       | 64.0          |
| PbO                            |                                |       | 20.0          |
| Na <sub>2</sub> O              |                                |       | 6.9           |
| K <sub>2</sub> O               |                                |       | 7.3           |
| Al <sub>2</sub> O <sub>3</sub> |                                |       | 1.9           |
|                                | Fe <sub>2</sub> O <sub>3</sub> |       | 0.07          |
|                                | P <sub>2</sub> O <sub>5</sub>  |       | 0.02          |
|                                | CaO                            |       | 0.07          |
|                                | SrO                            |       | 0.01          |
|                                | CeO <sub>2</sub>               |       | 0.22          |



**Table II.** Pb concentration in the filling solutions of RE1 and RE2 measured using ICP-MS.

| Reference electrode | Pb concentration ( $\mu\text{g/L}$ ) |
|---------------------|--------------------------------------|
| RE1                 | $\geq 500.000$                       |
| RE2                 | 31                                   |

To check whether RE1 used in this setup was actually responsible for the measured Pb contamination on the thin-film electrode, XRF was performed on the glass housing of the RE. Table I shows that the glass housing indeed contains a large amount of Pb (20 wt %), which by no means can be considered a trace amount. Additionally, ICP-MS was used to determine the Pb concentration of the filling solution (0.1 M KOH) of an unused RE1 as-received by the manufacturer (see Table II). Clearly, even 0.1 M KOH is able to leach out large quantities of Pb from the glass housing. These Pb contaminants would also end up in the electrolyte when RE1 would be employed directly in a three-electrode setup. This comes as a big surprise, as Hg/HgO reference electrodes are specifically designed to operate in alkaline solutions.<sup>14</sup>

**Contamination-free case (setup with RE2).**—Identical electrochemical measurements were performed on a second MgSc thin film using the setup containing RE2. Figure 6 shows the corresponding equilibrium curve and the potential response during each current pulse. This GITT experiment was performed using the same parameters as for the contaminated case, only during the last two pulses a current of +0.012 mA was used. Two observations can be made when comparing this case (Fig. 6) to the one shown in Fig. 2. First, the equilibrium data seem to be identical, except for the fact that in the contaminated case the storage capacity was 1700 mAh/g (Fig. 2), while it is only 1500 mAh/g in the contamination-free case (Fig. 6). This discrepancy can be explained by the fact that in the former case not only the oxidation of hydride is measured, but also the oxidation of deposited Pb contributes. This shows that inaccurate storage capacities can be measured if the setup contains a substantial level of contaminants. Second and more importantly, the potential response of the electrode during the current pulses shows a distinctly different behavior. The overpotential remains nearly constant throughout the entire discharge process and only increases when the thin film reaches its hydrogen-depleted state as expected. This clearly proves that the increase in overpotential in the initial case (shown in Fig. 2) is due to surface poisoning by Pb species.

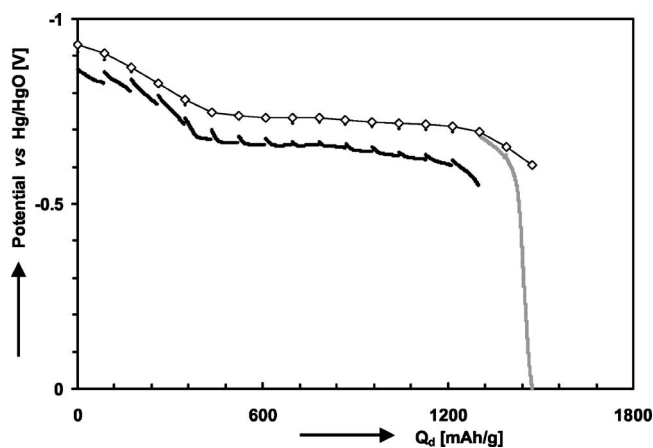


**Figure 6.** Electrochemical response of a thin-film electrode measured in a contamination-free setup. Other than the equilibrium curve of the material (◇), the potential responses during each GITT pulse are shown. Current used during the GITT pulses: +0.12 mA (bold line), +0.012 mA (gray line).

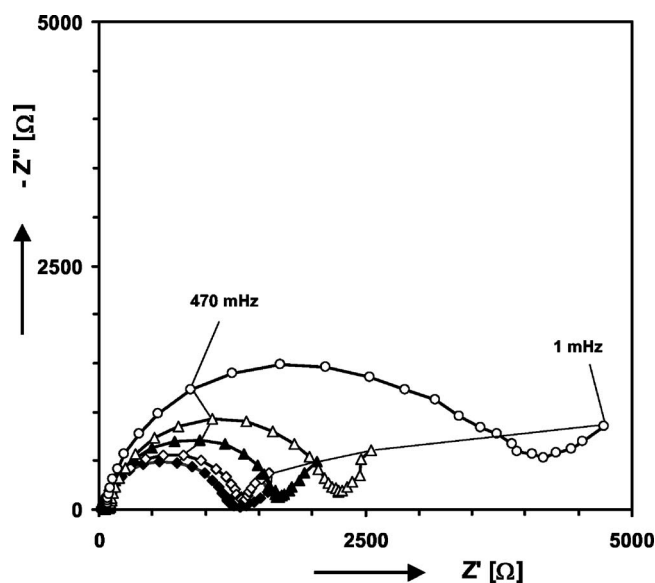


**Figure 7.** Impedance responses of a thin-film electrode, measured in a setup containing only trace amounts of contaminants, for different periods of continuous polarization at  $-0.925$  V. Polarization time: (◆) 0 days, (◇) 1 day, (▲) 2 days, (△) 3 days, and (○) 7 days.

As for the first case, the charge-transfer kinetics of the electrode was investigated while keeping the thin film at a constant potential of  $-0.925$  V (see Fig. 7). This time, as opposed to the impedance responses shown in Fig. 3, not only semicircular responses linked to kinetics are measured but also low-frequency responses linked to diffusion of hydrogen.<sup>15,16</sup> Focusing on the kinetics part, it is apparent that the magnitude of the impedance over time is more than one order of magnitude smaller than the contaminated case. Figure 4 shows  $R_{ct}$  and  $I_0$  plotted vs time for the contamination-free case (curve b). Interestingly, though to a much lower extent, a linear increase of  $R_{ct}$  can again be observed. From this it must be concluded that even in the contamination-free setup minor surface poisoning must have occurred. Additionally, when comparing curves a and b in Fig. 4, the  $R_{ct}$  at the start of the potentiostatic experiment (0 days) is not equal for both electrodes. The electrode measured in the contaminated setup (see Fig. 3) shows a value of  $2500 \Omega$ , whereas the  $R_{ct}$  of the second electrode, measured in the contamination-free setup, is only about  $1200 \Omega$  (see Fig. 7). This indicates that during the GITT measurement, which preceded the potentiostatic experiment, some surface poisoning had already occurred in the case of the contaminated setup.

To check which materials were deposited on top of the electrode, RBS was again utilized. Figure 8 shows the corresponding RBS spectrum, which essentially shows the same peaks as explained thus far in this paper. It can be seen that Pb was once more deposited (peak G), although in a much lower quantity ( $2.5 \times 10^{15}$  atoms Pb/cm<sup>2</sup>, corresponding to three monolayers). This inevitably means that even when no apparent Pb source is present, unavoidable trace amounts present in cell components in contact with the electrolyte can still be deposited. Looking at Fig. 5 and 8 more closely reveals that besides Pb, minute quantities of Fe and Zn were also deposited. These are indicated as peaks H and I, respectively, in the enlarged section in Fig. 8. Most likely, all these contaminants originated from the Duran glass from which the electrochemical cell was constructed. Therefore, if surface poisoning is to be avoided altogether, the electrochemical cell should be constructed from a completely inert material (e.g., Teflon).

Table III shows the composition of this glass measured with XRF. These results confirm the presence of trace amounts of these three elements in the glass. Fe and Zn apparently leach out from the Duran glass after prolonged contact with strong alkaline electrolyte

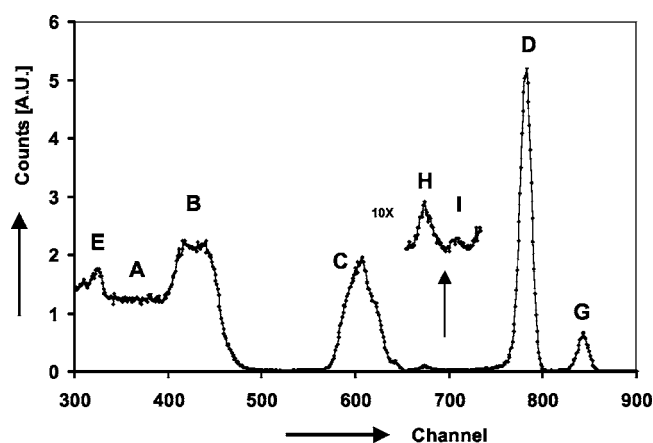


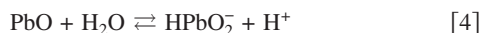
**Figure 8.** RBS spectrum of a thin-film electrode, measured in a contamination-free setup, after electrochemical characterization. The responses of interest can be attributed to: (A) quartz substrate, (B) Mg, (C) Sc, (D) Pd, (E) oxygen, (G) Pb, (H) Fe, and (I) Zn.

and are subsequently electrochemically deposited onto the thin-film electrode. As the filling solution (6 M KOH) of an unused RE2, as-received by the manufacturer, contains only a trace amount of Pb (see Table II), no significant poisoning is expected from this RE.

### Discussion

In order to accurately investigate the charge-transfer kinetics of thin-film electrodes it is crucial that the electrode/electrolyte interface remains unchanged throughout all experiments. In the case presented in this contribution, this interface consists of palladium (Pd) and KOH solution and the kinetics of this thin-film electrode are therefore directly linked to the amount of Pd present at this interface. If for some reason during experiments other materials are deposited onto the Pd, the kinetics will certainly be influenced.

Foreign material can be deposited from solution either chemically or electrochemically. This study, however, is limited to electrochemical deposition of lead (Pb). The Pourbaix diagram of Pb in aqueous solutions, depicted in Fig. 9, shows that PbO species in contact with strong alkaline solutions are unstable and mainly form dissolved  $\text{HPbO}_2^-$  ions according to<sup>17</sup>



This means that when RE1 is used in a three-electrode setup filled with an alkaline solution (i.e., KOH), Pb leaches out from the lead-glass housing and ends up as the dissolved  $\text{HPbO}_2^-$  species in the electrolyte. ICP-MS measurements have already confirmed that

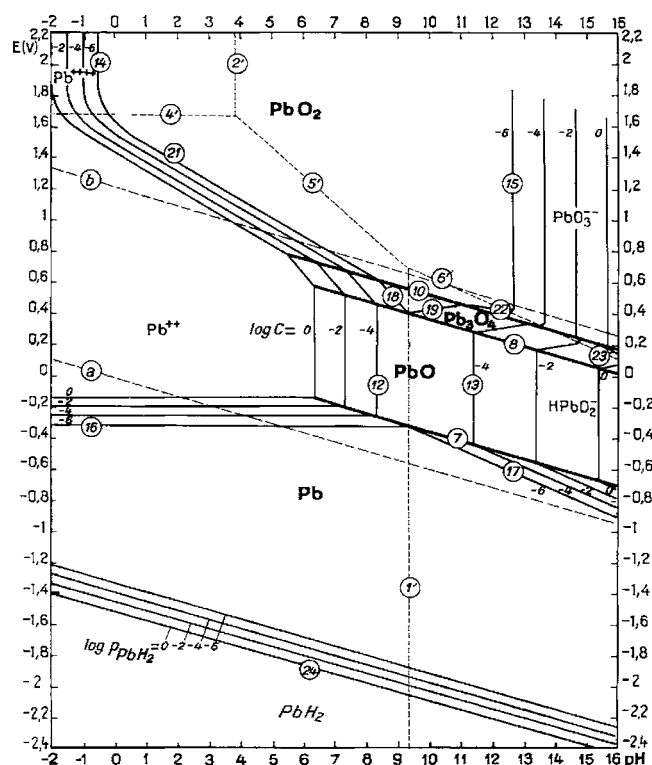
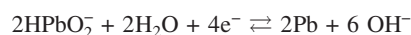


**Figure 9.** Pourbaix diagram of lead (Pb) in an aqueous solution in which the equilibrium potential vs a normal hydrogen electrode [V] is plotted vs pH.<sup>17</sup>

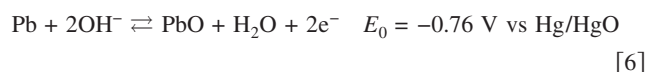
this happens experimentally (see Table II). As a chemical equilibrium exists between the dissolved and the solid species (see Eq. 4), the electrolyte within the setup is initially Pb-contaminated near the source only, in this case the RE. Over a long period of time, diffusion, migration, and convection ensure that the entire electrolyte will be contaminated, resulting in a uniform Pb concentration. It is interesting to note that the solubility of PbO in 6 M KOH, which corresponds to a pH of 15.46, is extremely high and theoretically amounts to a concentration of  $[\text{HPbO}_2^-] \approx 1 \text{ mol/L}$ .<sup>17</sup>

Once an appreciable  $\text{HPbO}_2^-$  concentration has been built up in the electrolyte, it can be electrochemically deposited or stripped during current flowing conditions. Figure 9 shows that at pH 15.46 and a potential range of 0 to -1.2 V vs Hg/HgO (which corresponds to standard conditions during hydrogen loading/unloading in this study),  $\text{HPbO}_2^-$  can theoretically be deposited as metallic Pb at potentials more negative than -0.74 V, according to



$$E_0 = -0.74 \text{ V vs Hg/HgO} \quad [5]$$

This would thus simultaneously occur with electrochemical hydrogen loading of the thin film (Reaction 1). During hydrogen extraction a combination of oxidation processes occurs. First, the metallic Pb covering the Pd topcoat can be oxidized to PbO at working electrode potentials according to



Additionally, the reverse of Reaction 5 can occur at potentials more positive than -0.74 V, converting metallic Pb back into  $\text{HPbO}_2^-$  species. Finally, when the electrode potential becomes more positive than 0 V, higher oxides like  $\text{Pb}_3\text{O}_4$  can be formed (see Fig. 9). This shows that the deposits covering the surface can be comprised of a mixture of metallic Pb and Pb oxides in varying ratios. The exact composition of these Pb deposits depends on the electrochemical

**Table III.** Composition of Duran glass measured by means of XRF.

| Main | Material                | Trace                   | Amount [wt %] |
|------|-------------------------|-------------------------|---------------|
|      |                         |                         |               |
|      | $\text{SiO}_2$          |                         | 78.0          |
|      | $\text{B}_2\text{O}_3$  |                         | 15.1          |
|      | $\text{Na}_2\text{O}$   |                         | 3.6           |
|      | $\text{K}_2\text{O}$    |                         | 0.6           |
|      | $\text{Al}_2\text{O}_3$ |                         | 2.5           |
|      |                         | $\text{Fe}_2\text{O}_3$ | 0.03          |
|      |                         | $\text{ZnO}$            | 0.007         |
|      |                         | $\text{PbO}$            | 0.01          |
|      |                         | $\text{MgO}$            | 0.015         |
|      |                         | $\text{P}_2\text{O}_5$  | 0.003         |
|      |                         | $\text{TiO}_2$          | 0.04          |
|      |                         | $\text{ZrO}_2$          | 0.03          |
|      |                         | $\text{BaO}$            | 0.01          |

potential of the thin-film electrode, the concentration of species participating in the electrochemical reactions, and the chemical equilibria of the dissolved and solid Pb species.

Deposits covering the thin-film electrode will, as mentioned before, severely influence the kinetics of the hydrogen adsorption reaction (Reaction 1). Depending on the material deposited, contaminants can alter the kinetics in two different ways. First, if the deposit is able to form a hydride itself and remains stable in alkaline solutions, the hydrogen adsorption reaction (Reaction 1) and absorption reaction (Reaction 2) manifest themselves at the Pd as well as the deposit. The rate at which Reaction 1 occurs depends on many different factors that are basically related to the specific compound and is therefore not the same at both materials. This, in turn, means that a mix of the kinetics at the Pd and at the deposit brings about the overall kinetic response of the thin-film electrode. This only holds if the overall kinetics of the hydrogen storage reaction is rate determined by Reaction 1 and not by the hydrogen absorption reaction (Reaction 2). As this study focuses on Pb deposits that are, under normal electrochemical conditions, not able to form hydrides themselves, a more detailed view on this possibility is omitted.<sup>17</sup>

The second scenario that can occur is that a material is deposited on top of the Pd, which is not able to form a hydride (in this case Pb). This implies that although Reaction 1 occurs at both the Pd (palladium) and the Pb (lead), Reaction 2 only occurs at the Pd. The kinetics of Reaction 1 can be described by the well-known Butler-Volmer equation<sup>13</sup>

$$I = I_0 \left[ \exp \left\{ \frac{-\alpha F \eta}{RT} \right\} - \exp \left\{ \frac{(1 - \alpha) F \eta}{RT} \right\} \right] \quad [7]$$

where  $I_0$  is the exchange current density,  $\alpha$  is the charge-transfer coefficient,  $R$  the gas constant,  $T$  the absolute temperature,  $F$  the Faraday constant, and  $\eta$  the overpotential. It is generally accepted that  $I_0$  is a crucial parameter in describing the kinetics of an electrochemical charge-transfer reaction. The relationship for  $I_0$  has been derived by Notten et al. and can be expressed as<sup>7,18</sup>

$$I_0 = F A_0 k_a^{(1-\alpha)} k_c^\alpha \theta^{y(1-\alpha)} (1 - \theta)^\alpha a_{\text{OH}^-}^{y(1-\alpha)} a_{\text{H}_2\text{O}}^z \quad [8]$$

where  $k_i$  are the rate constants of the electrochemical charge-transfer reaction (Reaction 1),  $A_0$  is the electrode surface area,  $\theta$  the surface coverage of  $\text{H}_{\text{ad}}$ ,  $a_{\text{OH}^-}$  and  $a_{\text{H}_2\text{O}}$  are the activities of the indicated electrolyte species at the electrode interface for which  $x, y, z$  are the reaction orders, respectively, and  $\alpha$  is the charge-transfer coefficient. The activities of both  $\text{OH}^-$  and  $\text{H}_2\text{O}$  can be considered as constant as diffusion limitations of these species in the electrolyte are negligible, which is reasonable due to the high concentrations in strong alkaline solutions. From Eq. 8 it is immediately clear that  $I_0$  depends linearly on  $A_0$ . As only part of the Pd surface is covered with Pb, the overall  $I_0$  of the system can be represented by the following relationship<sup>18</sup>

$$I_0 = K_{\text{I}} A_{0,\text{I}} k_{\text{I}} \theta_{\text{I}}^{x(1-\alpha)} (1 - \theta_{\text{I}})^\alpha + K_{\text{II}} A_{0,\text{II}} k_{\text{II}} \theta_{\text{II}}^{x(1-\alpha)} (1 - \theta_{\text{II}})^\alpha \quad [9]$$

where the subscripts I and II refer to Pd and Pb, respectively;  $K = F a_{\text{OH}^-}^{y(1-\alpha)} a_{\text{H}_2\text{O}}^z$  and  $k = k_a^{(1-\alpha)} k_c^\alpha$ . As the  $I_0$  of the charge-transfer reaction (Reaction 1) at Pb is many orders of magnitude lower than at Pd,<sup>19</sup> the second term on the right in Eq. 9 can effectively be neglected. This means that the overall  $I_0$  is completely dictated by the kinetics of the charge-transfer reaction at Pd. Inevitably, when surface poisoning progresses,  $A_0$  will diminish and therefore  $I_0$  as well.

By comparing the contaminated case (setup employing RE1) to the contamination-free case (setup employing RE2), it can clearly be demonstrated that dissolution of Pb contaminants from RE1 leads to a substantial concentration of  $\text{HPbO}_2^-$  in the electrolyte. This  $\text{HPbO}_2^-$  can subsequently be deposited electrochemically, leading to large differences in electrochemical response. The larger overpotential in the contaminated case (Fig. 2) as compared to the contamination-free case (Fig. 6) must be attributed to a higher  $R_{\text{ct}}$

due to Pb deposits on the surface. Figure 4 shows that for the contaminated case  $R_{\text{ct}}$  increases linearly with time when potentiostatically depositing Pb (curve a). This is caused by a reciprocal decrease in  $I_0$  brought about by a similar decrease in  $A_0$  (see Eq. 9). This reciprocal decrease of  $A_0$  in time can originate from the following two phenomena: First, when the exposed Pd surface diminishes (due to poisoning), the probability increases that Pb nucleates and starts to form new crystals onto already-poisoned areas instead of onto still-exposed Pd. Second, Pb is preferentially used to increase the size of existing Pb crystals that have been formed at an earlier stage. To a much lower extent, a linear increase of  $R_{\text{ct}}$  in time is also demonstrated by the contamination-free case (Fig. 4, curve b), which has to be linked to minor surface poisoning due to unavoidable trace amounts of contaminants in the setup.

The results discussed so far clearly point to the fact that accurately measuring the electrochemical response of MH thin-film electrodes is not straightforward. Due to their small surface area, thin films are sensitive to rapid surface poisoning, which severely influences the kinetic properties. It is clear that extreme care has to be taken in making sure that all cell components are of the highest purity and do not contain more than trace amount of impurities that can lead to poisoning. Although specifically designed to operate in alkaline solutions, the radiometer XR430 Hg/HgO RE (RE1) appeared to be an unexpected source of significant Pb contamination (see Fig. 2 and 5). Using a Pb-free RE (RE2), an accurate electrochemical response of the thin-film electrode could be measured (see Fig. 6 and 8). However, minor surface contamination could not be avoided when the electrode potential was set to  $-0.925$  V for a long period of time, up to 7 days (see Fig. 7). At this point it is important to note that during normal electrochemical characterization the potential of the thin-film electrode might be in the potential range where Pb deposition occurs only for a few hours. Therefore, the cases presented in this study are extreme examples and the actual decrease in kinetics (or  $I_0$ ), especially in the setup that only contained trace amounts of impurities, is much less than shown in Fig. 4 (curve b). Cross-correlation of the results presented in Fig. 4, 5, and 8 indicates that there seems to be a clear correlation between the amount of Pb deposited on the surface and the value of  $R_{\text{ct}}$ . When comparing the contaminated case to the contamination-free case, a ten times higher Pb concentration on the electrode surface (measured by means of RBS) resulted in an increase of  $R_{\text{ct}}$  by one order of magnitude (obtained from the impedance data).

## Conclusions

The effect of RE-induced surface poisoning of MgSc thin-film electrodes has been investigated. A comparison was made between the electrochemical responses of identical MgSc thin films measured in two different setups. One setup contained a radiometer XR430 Hg/HgO RE, which appeared to be commercially manufactured with a Pb-glass construction containing 20 wt % Pb. The second setup contained a Pb-free Hg/HgO RE from Koslow Scientific Company, constructed with a polyethylene housing. It was shown that Pb species originating from a radiometer Hg/HgO RE readily dissolved into the electrolyte. These dissolved species can be deposited electrochemically on the surface of thin-film electrodes, both as metallic Pb and Pb oxides, during electrochemical hydrogen loading/unloading of the MgSc alloy. Electrochemical measurements showed inferior charge-transfer kinetics when employing a radiometer RE as compared to the Koslow RE, which was linked to the deposition of Pb species on the electrode surface. Surface poisoning thus prevents accurate determination of kinetic parameters related to the hydrogen adsorption reaction. Furthermore, the electrode kinetics are directly linked to the amount of Pb deposits covering the thin film by combining EIS and analytical techniques. Additionally, Pb deposits covering the thin-film electrode cause deviations in the calculated hydrogen storage capacity that are too large to be ignored (up to 15%).

### Acknowledgments

The authors thank T. Raaymakers for the preparation of the thin films, T. Dao for the RBS analysis, J. Smulders for the MS-ICP measurements, and H. Jaspers for providing XRF data. Furthermore, P. Rommers and Y. Tamminga are acknowledged for many interesting and stimulating discussions.

*Eindhoven University of Technology assisted in meeting the publication costs of this article.*

### References

1. J. N. Huiberts, R. Griessen, J. H. Rector, R. J. Wijngaarden, J. P. Dekker, D. G. de Groot, and N. J. Koeman, *Nature (London)*, **380**, 231 (1996).
2. J. N. Huiberts, J. H. Rector, R. J. Wijngaarden, S. Jetten, D. de Groot, B. Dam, N. J. Koeman, R. Griessen, B. Hjorvarsson, S. Olafson, and Y. S. Cho, *J. Alloys Compd.*, **239**, 158 (1996).
3. P. H. L. Notten, M. Kremers, and R. Griessen, *J. Electrochem. Soc.*, **143**, 2990 (1996).
4. M. Ouwerkerk, *Solid State Ionics*, **113-115**, 431 (1998).
5. P. H. L. Notten, *Recent Res. Dev. Electrochem.* **3**, 1 (2000).
6. P. van der Sluis, M. Ouwerkerk, and P. A. Duine, *Appl. Phys. Lett.*, **70**, 2990 (1997).
7. P. H. L. Notten, M. Ouwerkerk, A. Ledovskikh, H. Senoh, and C. Iwakura, *J. Alloys Compd.*, **356-357**, 759 (2003).
8. P. H. L. Notten, M. Ouwerkerk, H. van Hal, D. Beelen, W. Keur, J. Zhou, and H. Feil, *J. Power Sources*, **129**, 45 (2004).
9. R. A. H. Niessen and P. H. L. Notten, *Electrochim. Acta*, **50**, 2959 (2005).
10. R. A. H. Niessen and P. H. L. Notten, *J. Alloys Compd.*, In press.
11. J. R. MacDonald, *Impedance Spectroscopy*, p. 74, John Wiley & Sons, New York (1987).
12. C. Gabrielli, P. P. Grand, A. Lasia, and H. Perrot, *J. Electrochem. Soc.*, **151**, A1925 (2004).
13. A. J. Bard and L. R. Faulkner, *Electrochemical Methods, Fundamental and Applications*, p. 100, John Wiley & Sons, New York (2001).
14. D. T. Sawyer and J. L. Roberts, *Experimental Electrochemistry for Chemists*, p. 48, John Wiley & Sons, New York (1974).
15. T.-H. Yang and S.-I. Pyun, *Electrochim. Acta*, **41**, 843 (1996).
16. C. Gabrielli, P. P. Grand, A. Lasia, and H. Perrot, *J. Electrochem. Soc.*, **151**, A1943 (2004).
17. M. Pourbaix, *Atlas of Electrochemical Equilibria in Aqueous Solutions*, 2nd ed., p. 496, National Association of Corrosion Engineers, Houston, TX (1974).
18. P. H. L. Notten and P. Hokkeling, *J. Electrochem. Soc.*, **138**, 1877 (1991).
19. T. Erdey-Grúz, *Kinetics of Electrode Processes*, p. 174, Adam Hilger, Ltd., London (1972).